Seam Welding Monitoring System Based on Real-Time Electrical Signal Analysis

A new approach to in-line seam welding quality evaluation is presented

BY MASSIMO LANZONI, MIRKO SALOMONI, AND BRUNO RICCÒ

ABSTRACT

This paper presents a novel welding quality evaluation approach based on the analysis of electrical signals. The method has been implemented in an automatic system developed using field-programmable gate array (FPGA) acquisition boards and custom software. The system has been implemented in an industrial machine to detect faults in tinplate welding. Experimental results show that the system is characterized by high sensitivity and high speed. Furthermore, it needs simple conditioning electronics and tuning procedures. The system is suitable for network operation and remote control.

Background

Industrial machines are generally parts of complex production systems where product quality must be automatically evaluated by means of several checks during intermediate fabrication steps. In recent years, the importance of reliable quality evaluation has greatly increased due to the reduction in production gain margins.

In this context, a typical step of a production line, which is sometimes responsible for important faults, is welding. Therefore, nondestructive and automatic methods to monitor welding quality are normally implemented. Depending on welding type and speed, the following methods are based on different techniques: visual (Refs. 1–5), ultrasonic inspection (Ref. 6), electrode distance (Ref. 7), and electrical (Refs. 8–13).

Unfortunately, in the case of the seam welding machines considered in this paper, none of the available techniques is applicable.

Visual inspection is based on the use of template matching techniques; in particular, images are captured after the welding process is completed, and processing algorithms are used to compare them with reference images (for example, Ref. 1, computing the cross correlation between the target image and a portion of the acquired one). In some cases, where faults may lead to catastrophic results, costly X-ray or γ-ray inspections are made, and the shape of the image density profile along the weld interface is analyzed (Ref. 3). These techniques, however, can be applied only when welding process times are compatible with the duration of suitable image processing. Furthermore, visual techniques are not applicable when the welding area is not visible, as is the case of interest for this work.

An alternative visual technique is based on the analysis of the welding temperature (Refs. 2, 5), measured in real time using an infrared sensor and welding torch control. In this case, however, at least one side of the welding area must be visible, and again this is not the case of the seam welding machines, where both sides of the welding point are masked by the welding tool.

Another parameter that can be observed for quality monitoring is the electrode displacement during welding (Ref. 7). Such a technique, however, is applicable only when the welding electrodes and the parts to be welded are fixed during the operation, which is not the case considered in this paper where the electrodes (hence, also the welding point) are constantly moving along a line.

In the specific case of seam welding, a fault is represented by a missing welded point segment, possibly due to a variety of reasons (misalignments of the parts to be welded, border defects, dust or oil on the welding area, and so on). In some cases (i.e., welding of cans), this type of defect may result in gas or liquid leakage, unacceptable in cans for pressurized gas (that must have zero welding defects) or only partially tolerable in cans for solids of high-viscosity liquids.

Modern seam welding machines can work at high speed (several m/s) and produce welding dots with dimensions in the order of 1 mm. As a result, thousands of welding dots per second must be analyzed and processed in real time. To monitor their quality at full speed, all the techniques mentioned previously (Refs. 1–7) are not applicable because they do not meet measurement speed and/or spatial resolution specifications. In particular, no method based on visual inspection (Refs. 1–5) can be used because a) welding takes place between two surfacing edges of thin plate; b) welding rollers mask the welding area; and c) complex signal processing algorithms are not compatible with the machine speed.

Furthermore, ultrasonic techniques such as those illustrated in Ref. 6 are also not applicable because a) the part to be inspected is not fixed with respect to a probe; and b) the resolution is too low.

As an alternative, real-time monitoring of seam welding quality can be achieved by capturing the waveform of welding current and electrode voltage to be compared with correct references, because defects produce anomalous electrical behavior.

This technique has been successfully implemented in the case of spot welding (Refs. 8–13) where electrodes remain in the same position during the whole welding period, lasting several inverter cycles (from 6 to 10). Because the inverter frequency is 60 Hz, under such conditions, the time interval available for measure-

KEYWORDS

Process Monitoring
Resistance Seam Welding
Quality
Welding Defects and Flaws
Signal Processing
Real Time
Virtual Instrumentation

MASSIMO LANZONI (massimo.lanzoni@unibo.it) and BRUNO RICCÒ are with DEIS University of Bologna, Italy. MIRKO SALOMONI is with Cevolani SPA, Bologna, Italy.

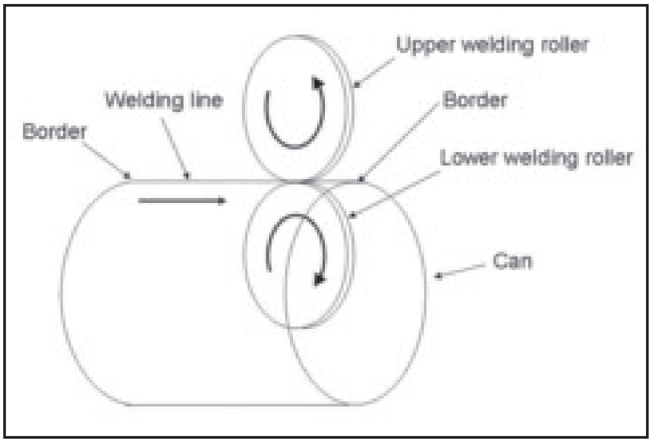

Fig. 1 — Working principle of the welding machine described in this work. The bent tinplate is driven between two welding rollers. Welding takes place in the contact area between the surfacing can edges (weld interface).

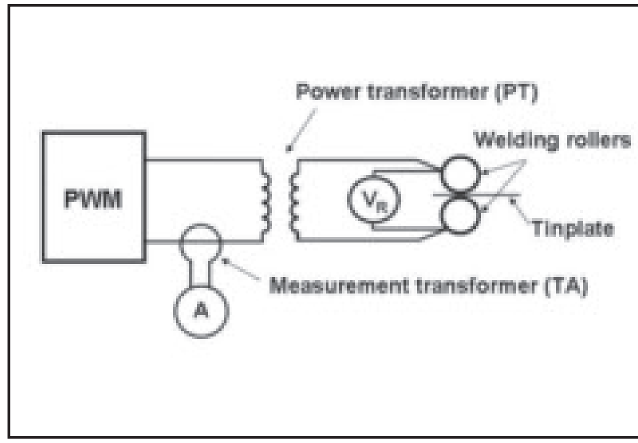

Fig. 2 — Electrical schematics of the welding machine power circuit. V_R represents the voltage between the welding rollers. The system features two transformers; one (TA) is used to measure the current flowing through the primary coil of the other (power) transformer (PT).

ments corresponds to 100–160 ms, and the shape of the resistance vs. time (in practice as a function of the inverter periods) is used (Refs. 10, 12) to decide about welding quality by comparing it with experimental or simulated reference data. Unfortunately, this approach is not applicable to the case of seam welding of interest in this work, essentially because the electrodes are moving along a (welding) line, and several points need to be welded in a short time. Each weld takes place in a single inverter semiperiod, near the current maximum value. Therefore, because in our case the inverter frequency is about 1 kHz, the resistance (or a related parameter) must be analyzed in a few hundreds of microseconds; thus, only a single (effective) resistance value, instead of a whole waveform, can be taken.

In this regard, a major point of our results is that they clearly show this information is sufficient to effectively detect defective welding.

In the case of seam welding, the approach based on analysis of voltage and current presents several specific and critical problems. First of all, as mentioned previously, analysis speed is much higher than in spot welding and requires dedicated high-speed signal analysis circuits. In this context, the conventional analog approach to signal analysis has several disadvantages because a) the system design is expensive, necessarily customized for a specific machine, difficult, and expensive to modify; and b) accurate and critical tuning is normally required. Alternatively, signals can be sampled and digitally processed in real time, but high-performance embedded systems based on digital signal processing (DSP) or field-programmable gate array (FPGA) devices are needed to meet machine speed specifications. Compared with its analog counterpart, the digital approach allows the modification or fine tuning of the system simply by acting on the system software, ideally without machine stopping, or the need of special equipment as well as trained personnel.

This paper improves the field introducing a new approach based on the combination of high-performance analog signal conditioning circuits and off-the-shelf advanced digital acquisition boards. The result is an advanced monitoring system featuring on-board signal processing that can be programmed with a high-level language (LabVIEW™). Consequently, algorithm modifications are simple and do not involve specific instrumentation. Furthermore, because the whole system is managed by a personal computer (PC), networking, remote control, and updating can be easily implemented.

To describe the developed system, this paper is organized by giving a brief description of the welding machine used as a target for this work; describing the architecture and main elements of the monitoring system; providing some details about software implementation; showing some experimental results; and ending with a final discussion.

Operation of the Welding Machine

The welding machine considered in this work is able to produce a sequence of welding points, called nuggets, along the edge of a tinplate suitable for can fabrication. The principle of the welding operation is illustrated in Fig. 1.

The tinplate is bent to form a cylinder, then the surfacing edges are welded by means of a couple of rolling electrodes connected to a power inverter. When the superimposed edges pass under them, high current flows between the rolling electrodes; thus, the temperature of the tinplate rises locally to high values, and welding takes place.

During this process, several types of inaccuracies localized in the border of the tinplate may lead to incorrect or missing welding. In particular, the presence of dust or oil can locally increase the resistance, modifying the electrical behavior of the system; holes in the tinplate can allow direct contact between electrodes; and random variations of the tinplate thickness, misalignment of the border to be welded, and/or local imperfections can significantly change the values of measured resistance. In all these cases, the mechanical characteristic of the nuggets produced in the defective area are different than the reference values and the results are weak. In all the cases mentioned, variations in the electrical behavior of the system during welding are produced. Structures appear in the waveforms of the current and the voltage between electrodes that can be used for fault detection.

Figure 2 presents a schematic representation of the electrical power circuit of the seam welding machine considered in this work.

A power inverter produces a dual polarity pulse width modulation (PWM) voltage signal to drive the primary coil of a power transformer (PT). The primary peak current is in the order of 50 to 150 A and is monitored by means of the current transformer (TA). The secondary of the PT is connected to the rolling electrodes, and the voltage across these (essentially the voltage drop on the resistance in the welding point) is monitored by means of sliding contacts. Welding current and voltage difference across the rollers are the two signals to be analyzed for welding quality evaluation. Their typical waveforms are shown in Fig. 3.

As can be seen, in spite of the impulsive behavior of the voltage across the rollers,

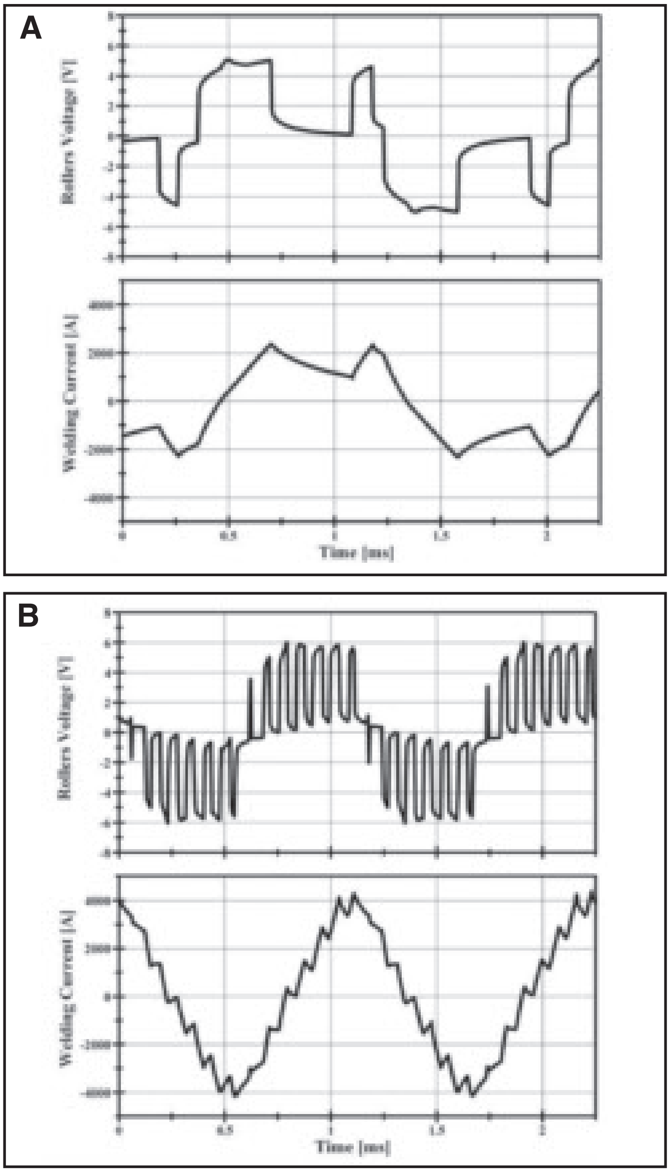

Fig. 3 — Typical primary current and roller voltage during welding. Different shapes of the PWM generator are used. A — The voltage across the rollers has few pulses and produces a quasi-triangular behavior of the current. B — The number of pulses (within a period) is larger, and the current has a quasi-sinusoidal shape.

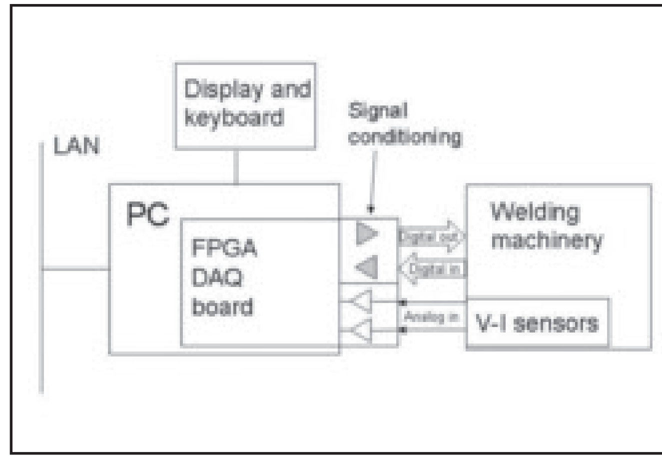

Fig. 4 — Schematic representation of the proposed welding monitoring system.

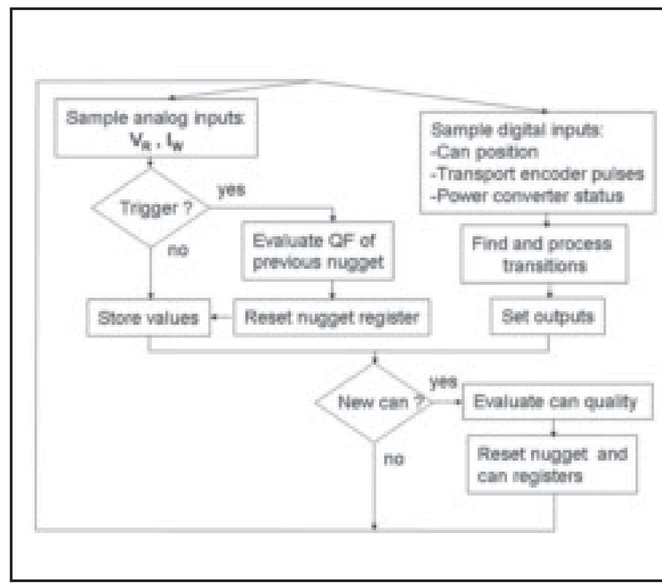

Fig. 5 — Schematic representation of the algorithm implemented in the FPGA, showing the parallel execution of analog and digital signal processing. Analog signal sampling and conversion takes about 4 μs. The whole cycle duration is 5 μs, corresponding to 200-k samples/s.

the welding current has a smoother shape due to the large inductance associated with the coils of the PT and secondary load. The peak value of the current flowing in the PT primary is in the order of 50 A, corresponding to a peak welding current of 2000–4000 A depending on the operating conditions (tinplate thickness, welding speed, and so on).

Because a nugget is produced both when the current reaches a maximum and minimum value, in the (typical) case of Fig. 3B, the duration of the welding period is about 0.7 ms.

In our monitoring system, the waveforms of Fig. 3 are sampled at 200-k samples/s; thus, a double set of about 140 samples must be processed in less than a welding period (0.7 ms). Such a high processing speed can be reached only by means of dedicated analog circuits or high-speed mixed analog/digital electronics.

As already anticipated, the latter options were chosen, which offer many advantages such as reduced custom design of both hardware and software, networking capabilities, and low cost.

The Proposed System

The monitoring system of this work, consisting of a high-speed section for real-time signal processing and digital unit for the management of defective cans, is based on a new family of acquisition boards featuring on-board FPGA devices able to perform real-time signal processing defined by algorithms written in a special version of LabVIEW™.

Figure 4 gives a schematic representation of the system.

A Windows®-based PC is used for system management, operator interface, network connection, data collection, and storage. The PC is equipped with a NI 7830 PCI acquisition board featuring a FPGA device that can be programmed to process in real time both analog and digital signals at 40 MHz clock rate, corresponding to a clock period of 25 ns. The hardware blocks inside the FPGA can be organized for parallel processing of several signals.

In our system, analog signals from the

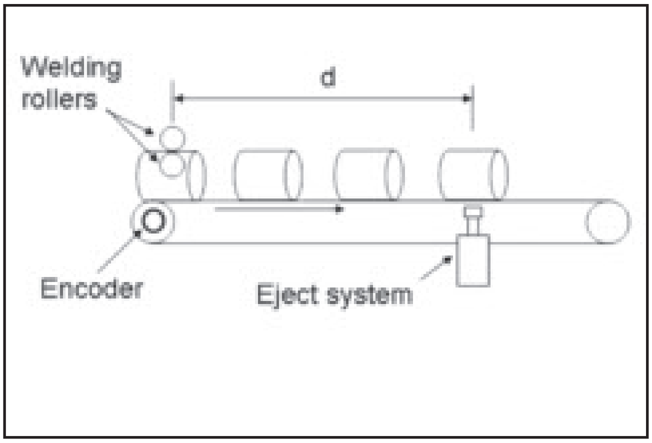

Fig. 6 — Schematic representation of the transport and ejection systems of the welding machine considered in this work.

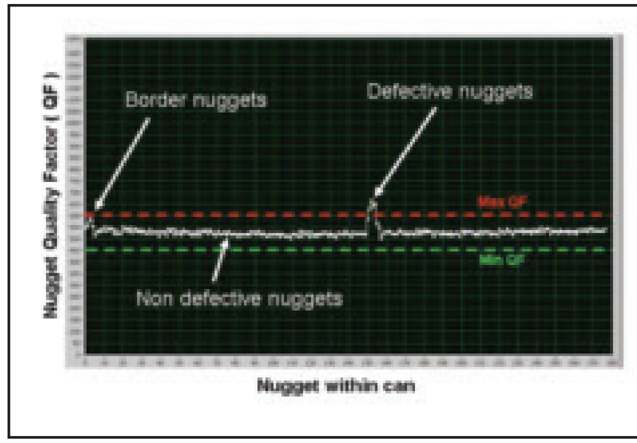

Fig. 7 — Results of the analysis of a single can. Each point in the figure represents the quality factor (QF) of a nugget along the weld interface. As can be seen, a set of nuggets exceeded the allowed thresholds (also see Fig. 8).

sensors (few, but needing time-consuming sampling and AD conversion) and many digital signals are processed in parallel. This allows performance of a whole sampling (AD conversion and partial processing cycle) in less than 200 clock periods (i.e., 5 μs in total), resulting in a 200-k cycles/s continuous operation of the algorithm.

Therefore, within a welding period of 0.7 ms, 140 16-bit digital samples of the analog signals are acquired and processed. This performance is sufficient to obtain suitable accuracy in welding quality evaluation, hence high resolution in defect detection.

A suitable signal conditioning stage has been designed to a) amplify analog signals from the sensors to fit the dynamics of the AD converters present on the FPGA board; and b) shift the level of the 24-V signals from digital sensors and actuators placed on the welding machinery to transistor-transistor logic (TTL) compatible levels. The gain of the top-quality amplifiers used for the analog channel can be varied to optimize the system for the particular machine to be monitored. Furthermore, the accuracy of signal sampling and conversion guarantees the effectiveness of the analysis even if the input signals do not completely span the converter dynamics. This is important from the point of view of system flexibility, because different signals (due to differences in tinplate thickness, welding current, and so on) can be treated without the need to adjust the conditioning amplifiers gain to any specific case.

As for software, the operator/network interface and system management program are written in LabVIEW™. The same holds for the FPGA program (slave), that, however, must be compiled and transferred to the FPGA before system operation.

Figure 5 shows a block diagram of the FPGA algorithm that represents the core of our system.

Two parallel data flows are implemented exploiting the parallel execution capability of the FPGA device. Starting when a new trigger event is detected (i.e., the current crosses the zero line while rising or falling), a new data collection is started. A loop consists in parallel sampling and conversion of the analog signals and sampling of digital inputs (can transport encoder pulses, new can synchronization signal, and so on). At each loop, the analog samples are stored and digital signals are processed. At the end of the welding period (i.e., when a new trigger event is detected), the collected analog samples are evaluated to obtain the nugget quality factor (QF) expressed by the average conductance (i.e., the reciprocal of the resistance) during a single welding period. The QF, determined by the current and voltage waveform during welding, is automatically compared with operator-defined limits, and if these are exceeded, a fault signal is produced and the faulty can is ejected. To avoid errors due to random noise superimposed to the current signal, a Schmitt trigger (realized via software) is used to detect the trigger event.

Product quality standards can be easily defined by the operator choosing the number of tolerable faults that depends on the application, because, for example, cans for aerosol normally require zero defects while those for solid contents are more tolerant. To manage this parameter, the operator can easily define/modify the limits for defect detection. This manual and empirical calibration is necessary because in real production environments, the process tolerances as well as the intrinsic randomness in fault nature and entity may easily lead to a different variance in a statistical data of good nuggets. Therefore, in some cases, the sensitivity of the system must be suitably adjusted to compensate for uncertainness in material characteristics.

To implement the ejection function by counting the transport encoder pulses, the FPGA algorithm evaluates the position of the welded cans within the transport system after the welding rollers and generates an expulsion command when a faulty can reaches the right position in front of the eject system — Fig. 6.

As can be seen in Fig. 6, a number of cans, depending on transport speed and tinplate format, is normally present within the transport system at the output of the welding point. Therefore, a set of registers containing the position of every can is required. These registers store the number of pulses of the transport encoder from the end of the welding and must be incremented (in parallel) at every encoder pulse. The eject system is activated if the can in the ejection position (corresponding to the fixed distance from the welding rollers) has been recognized as defective. Because real-time operation is needed, a portion of the FPGA is dedicated to updating and sampling the register's status.

Therefore, the FPGA is able to automatically manage both welding analysis and defective can ejection.

Furthermore, the quality of all the nuggets of the last welded can are stored in an internal memory, and the data can be transferred to the host program, without affecting the system operation, exploiting the direct memory access (DMA) option. These data provide important information to the operator (tinplate quality, adjustments to the machinery setup, and so on).

The main LabVIEW™ program (host), running on a PC, is dedicated to service tasks such as data collection and visualization, operator interface, network connection, and remote control of the monitor system. The main program panel allows the operator to view the data (of course, in compact form) concerning a set of cans.

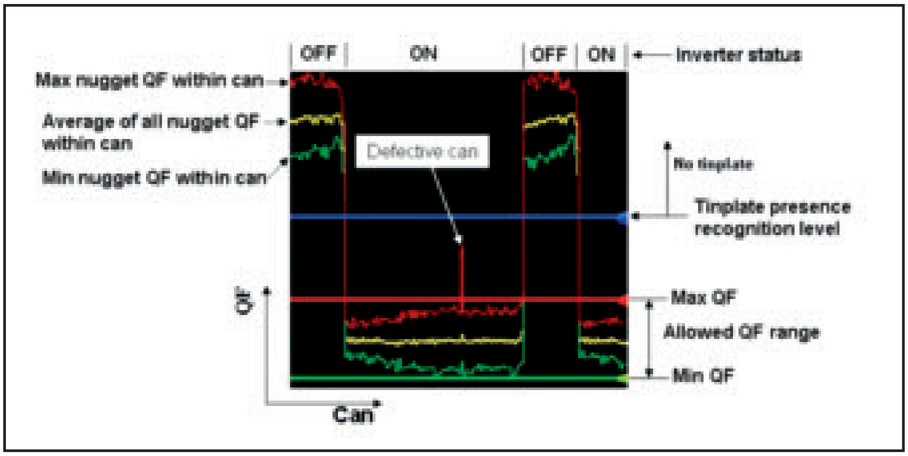

Fig. 8 — Example of welding analysis in the case of quasi-triangular welding current. Each point represents the result of the analysis of a set of nuggets within a can. The following three curves are displayed: The red and green curves represent the maximum and minimum values of QFs recorded during the analysis of the can while the yellow line represents the average of all the QFs. Defective welding leads to abnormal values that can be detected by comparison with thresholds indicated by the horizontal red and green dotted lines. Nondefective cans are characterized by maximum and minimum QFs within the range delimited by these thresholds. A third (blue) line indicates the threshold allowing detection of the absence of tinplate that produces high values of the QF. In this case, the welding machine inverter is instantly switched off to prevent electrode damage.

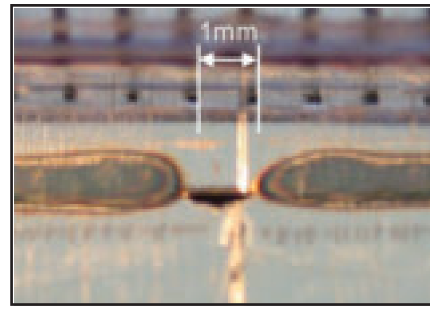

Fig. 9 — Example of defect due to border imperfection.

The minimum, maximum, and average values of QFs measured for each nugget of a single can are shown.

As stated above, the host program is able to manage data storage in the hard drive of the PC. Furthermore, the operator can store significant sets of analysis parameters corresponding to various situations of can size, tinplate characteristics, etc. These sets of parameters can be transmitted to the FPGA via the internal PCI bus without affecting the measurement speed.

Experimental Results

The proposed system has been successfully implemented in commercial welding machines. Different prototypes have been applied to machines presenting different characteristics such as the output waveform of the PWM inverter.

As already mentioned, the system speed is sufficiently high to allow data transfer from the FPGA to the main program via a DMA channel. Thanks to this feature, the operator can verify the distribution of QF values along the weld interface of a single can — Fig. 7. This is important to optimize the analysis, because nuggets near the borders present slightly different quality values compared to those in the center of the can. This leads to a widening of the min.-max. window and decreased analysis sensitivity.

Figure 7 presents the typical results of the analysis of nuggets along the weld interface of a single can welded using the waveforms presented in Fig. 3B. As can be seen, the QF is almost constant with the exception of a few nuggets located near the center of the can where a defect has been encountered, presenting QF exceeding the maximum QF threshold (red horizontal line) set by the operator. In the specific case in the figure, border nuggets (normally presenting slightly abnormal QF values) have acceptable QFs; in others, the threshold is exceeded. In any case, the operator can decide to exclude from the analysis border nuggets or apply for a different decision threshold.

In general, the welding regions can be subdivided in different areas to be analyzed with different sets of parameters. A typical subdivision of practical interest is the beginning, center, and end of the cans, with the borders featuring different values with respect to the center. In this way, the effects of the cans' borders on the final quality evaluation can be eliminated using specific sets of threshold values.

The operator also has the possibility of masking the analysis of the first and last nuggets. This feature is important to avoid mistakes due to the fact that the voltage waveform across the welding rollers is not synchronous with the beginning of the tinplate to be welded. Thus, the first and last nugget may feature incomplete welding; hence, their values must be discarded.

Figure 8 shows typical results of the analysis of a set of cans. Each point of the curves in this plot represents a synthetic evaluation of the QF analysis of a whole set of nuggets within a can. The yellow line represents the average of the QF values. As can be seen, the average is almost constant from sample to sample.

On the contrary, defects produce an abnormal value of the maximum or minimum QFs (red and green curves, respectively).

Through the main panel, the operator can easily set boundary levels for can selection calibrating the position of the maximum and minimum horizontal lines (thus, selecting an allowed range for QF values). In addition, the lack of tinplate to be welded can be easily recognized because QF assumes values well above the maximum limit (red horizontal line). This condition can be detected by comparing the minimum QF detected (green curve) with a third threshold level (blue horizontal line). If this latter is found below min QF, the system can immediately inhibit the welding machine inverter.

In the same way, insulation between rollers (not shown in the figure) can also be detected. Because this situation is also potentially dangerous for the PWM inverter, the FPGA immediately asserts a disable digital line that will be reset at the beginning of the next can.

The same analysis performed on a set of cans welded using quasi-sinusoidal current waveforms gives similar results in spite of the fact that the voltage across the rollers features a high number of pulses, hence the noise induced on the measuring system is higher.

Noise produces peaks in the current waveform and extra peaks in the voltage waveform. However, the analysis is not affected because the differential amplifiers used in the analog front end have a low slew rate limiting the effect of pulse noise. As a result, in the normal case (no faults), the QF presents only slightly higher dispersion around the mean value than the values obtained in the case of Fig. 3A. Thus, small defects are not masked by the noise.

Figure 9 shows a typical defect safely detected by the system of this work. In the case of the measurements presented in this section, the speed of the tinplate was 1.3 m/s, resulting in a distance between nuggets of 0.9 mm. Therefore, the defect shown in Fig. 9 results in two defective nuggets at most.

System Features

Calibration

The system developed in this work does not require critical calibration procedures. The main operation is to optimize the gain of the amplifiers used in the conditioning circuit to account for the characteristics of the particular machine where the monitor is installed. In fact, the signal at the output of the TA transformer can vary within a large interval depending on the machine, and the same holds for the voltage across the welding electrodes. Therefore, to exploit the acquisition board AD converter (ADC) dynamics, the peak values of the amplified signals must be maintained at about 80% of the converter range.

A further calibration concerns the synchronization of the transport and acquisition systems to be achieved, varying the delay between a mechanically produced electrical trigger and the beginning of the acquisition.

Both these procedures are made easy by the execution of special calibration programs.

Human Interface

The human-machine interface of the system presented in this paper has been carefully designed to allow nonskilled operators to perform basic operations by means of easy-to-use commands implemented on a touch screen.

Of course, operators with higher skills can log on the system and access extended features such as statistics and calibration procedures.

Network Integration

The monitor system of this work is suitable for network integration in the manufacturing system. The main program is written in LabVIEW™, which provides an integrated Web server allowing remote control. The system can be completely controlled from a remote workstation running any Web browser. This feature is useful for effective surveillance of the plant from a single location or to improve remote assistance in the case of faults.

Conclusions

This work presented a welding monitoring system able to detect faults in real time and with high sensitivity.

The system is based on measurements and processing of electrical signals from sensors placed on the welding transformer and electrodes.

Working prototypes of the system have been developed using commercial acquisition systems and high-quality conditioning electronics. Such prototypes have been implemented on commercial machines with excellent results.

The system is able to perform accurate analysis in real time and allows remote assistance, management, and data collection.

The system is based on widely available components and can be easily extended to include additional sensors.

References

1. Kim, S.-M., Lee, Y.-C., and Lee, S.-C. 2006. Vision based automatic inspection system for nuts welded on the support hinge. *Proc. IEEE SICE-ICASE Intl. Joint Conf. 2006*, Busan, Korea, pp. 1508–1512.
2. Govardhan, S. M., Wikle, H. C., Nagarajan, S., and Chin, B. A. 1995. Real-time welding process control using infrared sensing. *Proc. IEEE American Control Conf.*, Seattle, pp. 1712–1716.
3. Li, Y., and Liao, T. W. 1996. Weld defect detection based on Gaussian curve. *IEEE Proc. of the Twenty-Eighth Southeastern Symposium on System Theory*, pp. 227–231.
4. Kim, C.-H., Choi, T.-Y., Lee, J.-J., Suht, J., Parkt, K.-T., and Kangt, H.-S. 2006. Development of welding profile measuring system with vision sensor. *Proc. IEEE Sensors, EXCO*, Daegu, Korea, pp. 392–395.
5. Nagarajan, S., Benerjee, P., Chen, W. H., and Chin, B. A. Feb. 1992. Control of the welding process using infrared sensors. *IEEE Trans. Robotics and Automation* 8(1): 86–93.
6. Guangzhi, D., Tiequn, C., and Jiaxiang, X. 2007. Research on image resolution in ultrasonic imaging inspection of welding defect. *Proc. IEEE 8th Intl. Conf. on Electronic Measurements and Instruments (ICEMI2007)*, Xi'an, China, pp. 965–968.
7. Lin, Z., Zhang, Y., Chen, G., and Li, Y. 2004. Study on real-time measurement of nugget diameter for resistance spot welding using a neuro-fuzzy algorithm. *Proc. IEEE Intl. Conf. on Instrumentation and Measurement Technology (IMTC 2004)*, Como, Italy, pp. 2230–2233.
8. Savage, W. F., Nippes, E. F., and Wassel, F. A. 1978. Dynamic contact resistance of series spot welds. *Welding Journal* 57(2): 43-s to 50-s.
9. Chien, C. S., and Kennatey-Asibu Jr., E. 2002. Investigation of monitoring systems for resistance spot welding. *Welding Journal* 81(9): 195-s to 199-s.
10. Dickinson, D. W., Franklin, J. E., and Stanya, A. 1980. Characterization of spot welding behavior by dynamic electrical parameter monitoring. *Welding Journal* 59(6): 170-s to 176-s.
11. Livshits, A. G. 1997. Universal quality assurance method for resistance spot welding based on dynamic resistance. *Welding Journal* 76(9): 383-s to 390-s.
12. Cho, Y., and Rhee, S. 2002. Primary circuit dynamic resistance monitoring and its application to quality estimation during resistance spot welding. *Welding Journal* 81(6): 104-s to 111-s.
13. Cho, Y., and Rhee, S. April 2004. Quality estimation of resistance spot welding by using pattern recognition with neural networks. *IEEE Transactions on Instrumentation and Measurements* 53(2): 330–334.